VUV EMISSION OF KR_2 MOLECULES UNDER HIGH-CURRENT SLIDING DISCHARGE EXCITATION

A.Treshchalov[a], E. Jalviste[a], A. Smerechuk[b], G. Gerasimov[c], R. Hallin[b] and A. Arnesen[b]

a) Institute of Physics, University of Tartu, Riia 142, 51014 Tartu, ESTONIA
b) Uppsala University, Department of Physics, Box 530, S-751 21 Uppsala, SWEDEN
c) Vavilov State Optical Institute, Birzhevaja Line 12, 199034 St. Petersburg, RUSSIA

Abstract. Fast-pulsed high-current sliding discharge along the surface of sapphire plate is applied for the excitation of high-pressure Kr gas. Time behavior of the VUV emission from excimer molecules and main atomic species were monitored. Kinetics of the first and second Kr_2 continua in conditions of powerful pumping and high electron density are discussed. Experimentally it is revealed the importance of direct electron impact excitation of 0_u^+ and 1_u Kr_2^* states from weakly bound Kr_2 molecules in the 0_g^+ ground state and free collision pairs of Kr atoms at high pressure conditions.

1. INTRODUCTION

A variety of applications (lithography, photochemistry, disinfections, etc) require intense light sources in vacuum ultraviolet (VUV) spectral range. Rare gas excimers have been known to be one of the most efficient VUV continuous radiation sources. For instance a dielectric barrier surface discharge in rare gas mixtures has conversion efficiency of about 60% (VUV light output from the discharge input electrical energy). Although lasing on these molecules was demonstrated long time ago, only few successful attempts to design discharge-excited lasers are reported [1]. Thus, designing and optimization of discharge-excited rare gas excimer lamps and lasers is an important and demanding task.

2. EXPERIMENTAL

Since the discharge in high-pressure inert gases tends to constrict due to ionization and thermal instabilities, specially designed fast discharge circuits should be used to avoid the constriction and to achieve high-efficient VUV emission. Figure 1 presents configuration of electrodes used in our sliding discharge. High voltage electrode (copper foil with a thickness of 0.1 mm) is placed between two grinded sapphire dielectric plates of 250×80×0.6 mm^3 (L×W×H) and pressed between two thick (10 mm) aluminum ground electrodes. This construction (a flat transmission line) plays also the role of extremely low-inductance peaking capacitor (C ≈ 3.5 nF) for the discharge.

The discharge electrical driving circuit is a thyratron-switched charge-transfer scheme with storage and peaking capacitors of 1.5 and 3.5 nF, respectively. The circuit permits a steep (~ 30 ns) voltage growth (~$3 \cdot 10^{11}$ V/s) at relatively low charging voltage (up to 20 kV). A sliding discharge is developed in two stages [2]: I - the running of direct ionization wave on the dielectric surface from the HV to the ground electrodes. This low-current prebreakdown is initiated during the rise of the voltage on the HV electrode by spatially uniform displacement currents, which are capacitively distributed along the electrode length. Stage II is a high-current back-running fast excitation wave. This stage, characterized by maximum deposition power, starts since the arrival of the excitation wave I to the ground electrode and the energy from a low-inductive peaking capacitor is deposited into the well-preionized plasma

[a] Electronic address: *atr@fi.tartu.ee*

sheet. The existence of the second stage is the main advantage of a sliding discharge over well-known surface barrier discharge, which is self-terminated after the development of the first stage.

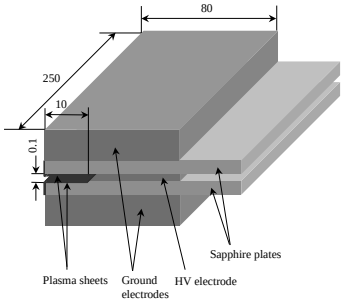

Figure 1. Schematic of the sliding discharge electrodes. Spontaneous emission from two arc-free plasma sheets (250x10x0.03 mm) is measured in the direction of the long axis.

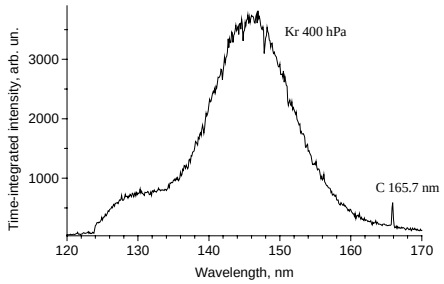

Figure 2. Time-integrated emission spectrum of a sliding discharge at a Kr pressure of 400 hPa.

Pulse repetition rate of our discharge device (up to 300 Hz) is limited mainly by the high voltage power supply. Gas mixture is effectively cooled on the surface of dielectric substrates between the excitation shots and no special gas circulation is necessary.

Spontaneous emission from the discharge plasma is detected through the output MgF_2 window by a normal-incidence 1 m vacuum monochromator with spectral resolution of 0.04 nm. Kinetics of emission were measured by the fast PMT (Hamamatsu R 1220) and the 400 MHz Tektronix 380 digitizer connected with a computer. Time-integrated emission spectra were measured by monitoring the PMT photocurrent pulse with sensitive pulse integrator. The discharge chamber (volume of ~5 l), made of stainless steel, and relevant gas handling system were evacuated by turbomolecular pumping system to 10^{-4} Pa. Kr and Xe gases with 99.998 % purity were used in our experiments.

3. RESULTS AND DISCUSSION

Figure 2. shows a typical time-integrated emission spectrum of a sliding discharge at Kr pressure of 400 hPa. The emission is known to originate from 0_u^+ and 1_u states of Kr_2 (see Figure 3.). The region of the intensity maximum (~146 nm), called the second continuum, corresponds to the low vibronic levels of Kr_2, but the blue and red shoulders, called the first continuum, originates from high vibronic levels of 0_u^+ and 1_u states.

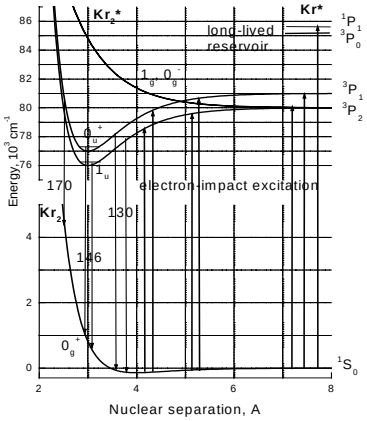

Figure 3. Kr atomic levels and simplified potential curves for Kr_2 molecules. Electron-impact excitation and spontaneous emission transitions (wavelengths in nm) are indicated.

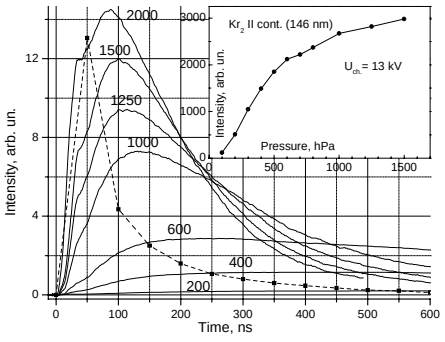

Figure 4. Time-resolved emission intensity of the second Kr_2 continuum (146 nm) in sliding discharge at different pressures (hPa). Dashed line is a time behavior of Kr^* 587 nm emission line, measured at 1250 hPa. The inset shows time-integrated intensity of the second Kr_2 continuum at different pressures at a fixed charging voltage (13 kV).

We also observed an additional broad continuum (200-400 nm) centered around 280 nm, which follows the discharge pumping pulse in its temporal behavior (see Figure 6.). We interpret this continuum as free-free transitions of electrons in collisions with neutral krypton atoms (bremsstrahlung continuum). The intensity of this continuum is proportional to densities of electrons and Kr.

Figure 4. presents time-resolved emission intensity of the second Kr_2 continuum (146 nm) in a sliding discharge at different gas pressures. Dashed line is a time behavior of Kr^* 587 nm emission line, measured at 1250 hPa. The intensity of this line follows the recombination flow in the afterglow.

The inset shows time-integrated intensity of the second Kr_2 continuum measured at different pressures at a fixed charging voltage (13 kV). The growth of the emission is caused mainly by the growth of the breakdown voltage of the discharge along with a pressure increase. Each pressure point has its specific voltage where the pumping efficiency achieves optimum. It means that maximum energy should be loaded to the sliding discharge from the fast pumping contour with low-inductance peaking capacitor and minimum energy should be dissipated into the plasma from the slow thyratron contour (storage capacitor). Figure 4. shows that even if the time-integrated intensity is close to the saturation at high pressures, the peak intensity continuously increases with pressure due to the compression of kinetics in time.

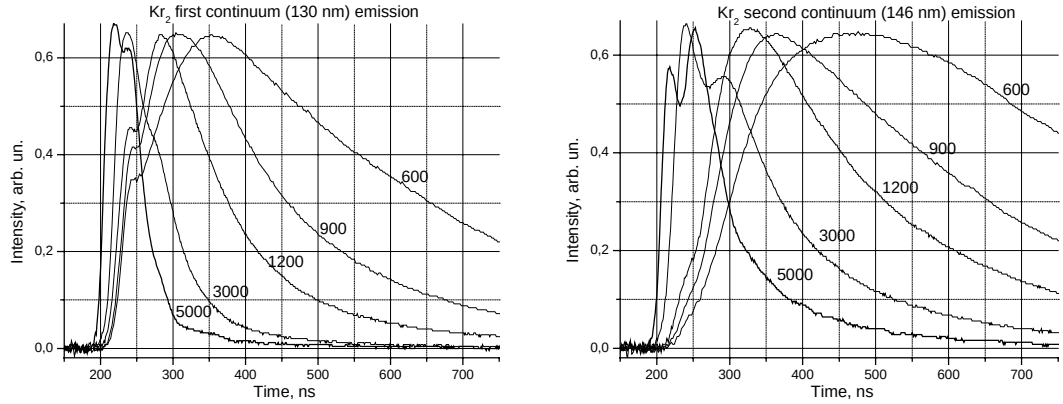

Figure 5. Time-resolved emission (normalized intensity) of the first (130 nm) and the second (146 nm) Kr_2 continua at different gas pressures (hPa). Discharge pumping pulse (FWHM) is about 20 ns.

Figure 5. presents time dependencies of the emission of the first (130 nm) and the second (146 nm) continua at different pressures of Kr. Maxima of all curves are normalized for better visualization.

The curves of these continua start with a rising edge, which becomes steeper with an increase of pressure. A small peak which is more pronounced on the curves of the first continuum appears on the rising edge of emission kinetics. Its magnitude increases with pressure (see Figure 6.). We associate the timing of the first peak with the discharge pumping pulse, whose duration is about 20 ns. The second maximum, being shallow at low pressures, and becoming sharper at higher pressures, we attribute to the population of Kr_2 0_u^+ and 1_u states via the cascade of reactions starting from recombination of Kr_2^+ ions (traditional mechanism). We also recorded the emission at 170 nm. According to [3,4] manifold of medium-high vibronic levels from 0_u^+ and 1_u Kr_2 states give their contribution to this emission. The time dependences of 170 nm emission are similar to that of 130 nm, but the first maximum is higher (see Figure 7.). Furthermore, according to [5], the radiative decay of higher vibronic levels in 1_u Kr_2 state is faster than for the lower levels. Indeed, in Figure 7. the decay time of 170 nm curve is longer than that of 130 nm. Thus, the presence of intense initial peak of the 170 nm curve indicates that corresponding intermediate vibronic levels of 0_u^+ and 1_u Kr_2^* states are effectively excited by direct electron impact of weakly bound Kr_2 molecules in the 0_g^+ ground state and free collision pairs of Kr atoms. This excitation mechanism can be used for more efficient production of VUV photons than for traditional method based on the recombination mechanism.

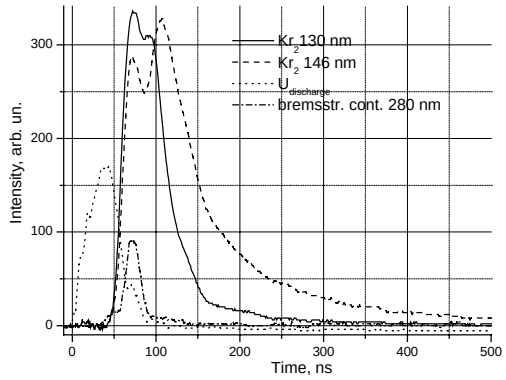

Figure 6. Time behaviors of the discharge voltage, Kr_2 the first (130 nm),the second (146 nm) and bremsstrahlung (280nm) continua at pressure of 5000 hPa.

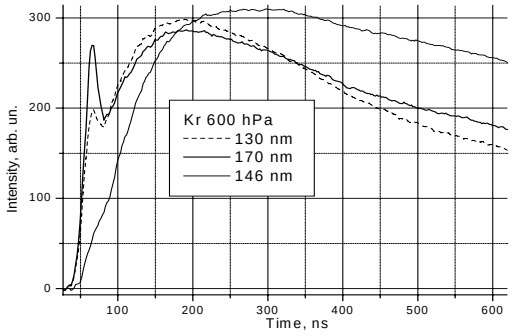

Figure 7. Time-resolved emission of the first (130, 170 nm) and the second (146 nm) Kr_2 continua at gas pressure of 600 hPa.

Rising the pressure accelerates the decay for both the first and the second continua (see Figure 5.). This pressure effect is described by two- and three-body reactions, which populate the emitting levels of Kr_2^*. Faster kinetics of the first continuum in comparison with the second continuum we explain by the fact that higher vibronic levels decay by vibrational relaxation as well as radiatively, but the lowest levels can decay only radiatively. At pressures larger that 1000 hPa the decay of both continua is non-exponential, where faster decay continuously transforms to the slower one (see Figure 5.) during the afterglow. It seems that at higher pressures the increased rate of collisional energy transfer processes is responsible for the faster component of decay in the mid-afterglow stage, but the disscociative recombination rate is responsible for the slower component in the far-afterglow.

For better understanding of the kinetics we calculated the time dependence of the second continuum using the experimental time dependence of the first continuum as a source function. This was realized by a differential equation $d[Kr_2II]/dt = [Kr_2I]/\tau_1 - [Kr_2II]/\tau_2$, where the $[Kr_2I]$ is the experimental curve of the first continuum, τ_1 is the vibrational relaxation time of higher vibronic levels and τ_2 is the effective radiative decay time of low vibronic levels. τ_2 is adjusted until the calculated and the measured time dependences of $[Kr_2II]$ are matched. The value of τ_1 almost did not affect the shape of the curves until $\tau_1 << \tau_2$ is valid.

For all the measured curves at different pressures the observed delay between the maxima of the first and the second continua as well as somewhat more rounded shape of the features of the second continuum in comparison with that of the first continuum was correctly reproduced. For pressure lower than 1000 hPa the agreement between calculated and observed $[Kr_2II]$ was good with $\tau_2 = 140$ ns. For higher pressure the modeling of the maximum intensity region required much smaller τ_2 (about 30 ns) than the tail (about 140 ns) of the $[Kr_2II]$ curve. This indicates that the effective decay rate of the emitting states of the second continuum decreases continuously with time during the afterglow. We interpret this effect by the mixing of 1_u and 0_u^+ states by electrons, whose density is decreasing in time. Complete mixing by electrons leads to the population of triplet 1_u state three times more than the population of singlet 0_u^+ state. In that case the apparent radiative lifetime, derived from known lifetimes of 1u and 0_u^+ (264 and 3.4 ns, respectively [6]), is 13 ns. Our analysis revealed that the decay time of the tail (about 140 ns) is almost pressure-independent in the range of 300-4000 hPa, but still much smaller than lifetime of 1_u (264 ns), obtained from measurements with synchrotron radiation excitation [6]. Again, the shorter lifetime we explain by partial collisional mixing with electrons in the discharge far-afterglow stage. At this final stage of the discharge the density of electrons is determined by the dissociative recombination, where the concentration of electrons and dimer ions Kr_2^+ are equalized. At electron densities between 10^{12} and 10^{13} cm^{-3} the dissociative recombination rate, being proportional to the squared density of electrons, is relatively slow and the density of electrons can be regarded as nearly constant during the time scale of few hundreds ns. This explains, why our value of

τ_2 seems to be not sensitive to the pressure.

We also interpreted the observed pressure dependence of the time behavior of the first continuum. After the fast discharge pulse the lowest $^3P_2$ and $^3P_1$ states of Kr as well as the molecular Kr_2 states emitting the first continuum, are populated by collisional energy transfer from $^1P_1$, $^3P_0$ (and higher atomic states of Kr) which can be treated as a long-lived reservoir (see Figure 3.). We found, that the two-body rate constant of collisional quenching of $^1P_1$ state in pure Kr (4×10^{-13} cm^3/s [7]), describes very well our pressure dependence of the decay rate of the first continuum in the mid-afterglow stage (the exponential decay at pressures <1000 hPa and the faster component of the non-exponential decay at pressures >1000 hPa). This rate-limiting two-body reaction simplifies significantly the kinetic modeling of fast high-pressure discharges in krypton.

ACKNOWLEDGMENTS

This work was supported by the Estonian Science Foundation under grant no. 5044 and The Royal Swedish Academy of Sciences.

REFERENCES

[1] Sasaki W. at all, *Optics Letters*, **26**, pp. 503-3 (2001)
[2] Treshchalov A. and Bashkin V., Spectroscopic diagnostics of sliding discharge as an efficient excitation source for high-pressure gas mixtures. In: *Proc. 6 th Int. Symp. On High Pressure Low Temperature Plasma Chemistry*, Cork, Ireland, 1998, pp. 298-302.
[3] Gerasimov G and Krylov B., *J. Opt. Technol.*, **62,** pp.362-4, (1995)
[4] Gerasimov G.at all, *Appl. Phys*, **B 66,** pp. 81-10 (1998)
[5] Madej A. and Stoicheff B., *Phys. Rev A*, **38**, pp.3456-9 (1988)
[6] Bonifeld T. at all, *Chem Phys. Letters*, **69,** pp. 290-7 (1980)
[7] Cook J. and Leichner P., *Phys. Rev. A*, **31,** pp. 90-9 (1985)